# Distinct molecular mechanisms of *HTRA1* mutants in manifesting heterozygotes with CARASIL

Hiroaki Nozaki, MD, PhD*
Taisuke Kato, PhD*
Megumi Nihonmatsu, MMed
Yohei Saito, MMed
Ikuko Mizuta, MD, PhD
Tomoko Noda, MD
Ryoko Koike, MD, PhD
Kazuhide Miyazaki, MD
Muichi Kaito, MD, PhD
Shoichi Ito, MD, PhD
Masahiro Makino, MD, PhD
Akihide Koyama, MMed
Atsushi Shiga, PhD
Masahiro Uemura, MD
Yumi Sekine, MD, PhD
Ayuka Murakami, MD
Suzuko Moritani, MD, PhD
Kenju Hara, MD, PhD
Akio Yokoseki, MD, PhD
Ryozo Kuwano, MD, PhD
Naoto Endo, MD, PhD
Takeshi Momotsu, MD
Mari Yoshida, MD, PhD
Masatoyo Nishizawa, MD, PhD
Toshiki Mizuno, MD, PhD
Osamu Onodera, MD, PhD

Correspondence to Dr. Onodera: onodera@bri.niigata-u.ac.jp

**Supplemental data at Neurology.org**

## ABSTRACT

**Objective:** To elucidate the molecular mechanism of mutant HTRA1-dependent cerebral small vessel disease in heterozygous individuals.

**Methods:** We recruited 113 unrelated index patients with clinically diagnosed cerebral small vessel disease. The coding sequences of the *HTRA1* gene were analyzed. We evaluated HTRA1 protease activities using casein assays and oligomeric HTRA1 formation using gel filtration chromatography.

**Results:** We found 4 heterozygous missense mutations in the *HTRA1* gene (p.G283E, p.P285L, p.R302Q, and p.T319I) in 6 patients from 113 unrelated index patients and in 2 siblings in 2 unrelated families with p.R302Q. The mean age at cognitive impairment onset was 51.1 years. Spondylosis deformans was observed in all cases, whereas alopecia was observed in 3 cases; an autopsied case with p.G283E showed arteriopathy in their cerebral small arteries. These mutant HTRA1s showed markedly decreased protease activities and inhibited wild-type HTRA1 activity, whereas 2 of 3 mutant HTRA1s reported in cerebral autosomal-recessive arteriopathy with subcortical infarcts and leukoencephalopathy (CARASIL) (A252T and V297M) did not inhibit wild-type HTRA1 activity. Wild-type HTRA1 forms trimers; however, G283E and T319I HTRA1, observed in manifesting heterozygotes, did not form trimers. P285L and R302Q HTRA1s formed trimers, but their mutations were located in domains that are important for trimer-associated HTRA1 activation; in contrast, A252T and V297M HTRA1s, which have been observed in CARASIL, also formed trimers but had mutations outside the domains important for trimer-associated HTRA1 activation.

**Conclusions:** The mutant HTRA1s observed in manifesting heterozygotes might result in an impaired HTRA1 activation cascade of HTRA1 or be unable to form stable trimers.
***Neurology*® 2016;86:1964–1974**

## GLOSSARY

**CARASIL** = cerebral autosomal recessive arteriopathy with subcortical infarcts and leukoencephalopathy; **cDNA** = complementary DNA; **CSVD** = cerebral small vessel disease; **FITC** = fluorescein isothiocyanate; **HTRA1** = high temperature requirement serine peptidase A1; **RANKL** = receptor activator of nuclear factor kappa-B ligand.

Cerebral autosomal recessive arteriopathy with subcortical infarcts and leukoencephalopathy (CARASIL), an autosomal recessive inherited cerebral small vessel disease (CSVD), involves severe leukoaraiosis, multiple lacunar infarcts, early-onset alopecia, and spondylosis deformans without hypertension.[1–4] High-temperature requirement serine peptidase A1 (*HTRA1*) gene mutations cause CARASIL by decreasing HTRA1 protease activity.[5] Although CARASIL is

*These authors contributed equally to this work.

From the Department of Medical Technology, School of Health Sciences, Faculty of Medicine (H.N.), Department of Molecular Neuroscience, Resource Branch for Brain Disease, Brain Research Institute (T.K., A.Y., O.O.), Department of Neurology, Clinical Neuroscience Branch, Brain Research Institute (M. Nihonmatsu, Y. Saito, A.K., A.S., M.U., Y. Sekine, M. Nishizawa), Department of Regenerative and Transplant Medicine, Division of Orthopedic Surgery (N.E.), and Department of Molecular Genetics, Bioresource Science Branch, Brain Research Institute (R. Kuwano), Niigata University, Niigata City; Department of Neurology (I.M., T. Mizuno), Kyoto Prefectural University of Medicine; Department of Neurology (T.N.), Ichinomiya Municipal Hospital, Aichi; Department of Neurology (R. Koike), Nishi-Niigata Chuo National Hospital, Niigata; Department of Neurology (K.M.), Shiseikai-Daini Hospital, Tokyo; Department of Neurology (M.K.), Kanazawa Medical University, Ishikawa; Department of Neurology (S.I.), Chiba University; Department of Neurology (M.M.), Nantan General Hospital, Kyoto; Departments of Neurology (A.M.) and Advanced Diagnosis (S.M.), Nagoya Medical Center, Aichi; Department of Neurology (K.H.), Japanese Red Cross Akita Hospital; Department of Internal Medicine (T. Momotsu), Sado General Hospital, Niigata; and Institute for Medical Science of Aging (M.Y.), Aichi Medical University, Japan.

Go to Neurology.org for full disclosures. Funding information and disclosures deemed relevant by the authors, if any, are provided at the end of the article.

a recessive inherited disease, for some *HTRA1* mutations, the parents of the probands with CARASIL present mild to severe white matter lesions.[6–8] Very recently, heterozygous mutations in *HTRA1* were identified in 11 families with CSVD[9]; so far, most of the parents of patients with CARASIL with *HTRA1* missense mutations, who are assumed to be heterozygotes, did not show symptomatic CSVD.[5–8,10–14] Moreover, heterozygotes carrying the p.R302ter or p.R370ter mutations, in whom residual HTRA1 activity might be near 50% that of controls, did not show symptomatic CSVD.[5,15] Because CSVD is frequently observed in elderly individuals,[16] it is, therefore, unclear which mutants truly contribute to CSVD pathogenesis and how HTRA1 mutants cause CSVD in heterozygous individuals. Here, we found heterozygous mutations in the *HTRA1* gene in individuals with CSVD and investigated the differences in biochemical characteristics between these mutant HTRA1s and mutant HTRA1s observed in homozygotes.

## METHODS

**Standard protocol approvals, registrations, and patient consents.** We recruited 113 unrelated Japanese index CSVD patients (table e-1 on the *Neurology*® Web site at Neurology.org) from 60 neurology centers in Japan between January 2009 and January 2014 using the following criteria: neurologic symptoms (stroke-like episodes, dementia, or gait disturbances); younger than 70 years; Fazekas deep white matter hyperintensities score of 3 on T2-weighted brain MRI[17]; and no pathologic mutations in the 2 to 24 exons of the *NOTCH3* gene, which is the causative gene for cerebral autosomal-dominant arteriopathy with subcortical infarcts and leukoencephalopathy. Forty-six patients (40.7%) had one or more first- or second-degree relatives with ischemic stroke. In-house Japanese control participants included 190 participants aged 74–90 years with no dementia, as evaluated by the Mini-Mental State Examination, and 130 participants aged 65–89 years with Fazekas deep white matter hyperintensities scores less than 2. Cervical and lumbar MRI were obtained from 3 patients with *HTRA1* mutations. Spondylosis deformans was diagnosed by focal osteophytes and severe degeneration of discs with canal stenosis. We obtained written informed consent from all individuals. The Institutional Review Board of Niigata University approved this study.

**Sequence analysis of *HTRA1* gene.** We isolated genomic DNA from peripheral lymphocytes. The primer pairs for the *HTRA1* and *NOTCH3* genes are listed in table e-2. Total RNA was isolated from whole blood from member II-4 of family 1, II-2 of family 4, and II-3 of family 5 and complementary DNA (cDNA) was synthesized with the use of a high-capacity cDNA reverse transcription kit (Applied Biosystems, Foster City, CA). Sequencing was performed using the BigDye® Terminator v3.1 cycle sequencing kit (Applied Biosystems) and ABI3130xl genetic analyzer (Applied Biosystems).

**HTRA1 protease assay.** We subcloned C-terminus $His_6$-tagged full-length wild-type HTRA1 or each C-terminus myc-$His_6$-tagged mutant HTRA1 cDNA into the pcDNA 3.1 vector (Invitrogen, Carlsbad, CA). The S328A HTRA1, which introduced a mutation in the protease active site of HTRA1, was used as a negative control.[18] We cotransfected equal molar amounts of mutant and wild-type HTRA1 cDNA expression vectors into FreeStyle 293 cells (Invitrogen). After 48 hours of incubation, each HTRA1 recombinant protein was purified from the cell culture conditioned media using a HisTrap FF crude column (GE Healthcare, Cleveland, OH). After preincubating 1 μg of purified protein at 37°C, we evaluated wild-type and mutant HTRA1 protease activities using fluorescein isothiocyanate (FITC)–labeled casein as a substrate (Fluorescent Protease Assay Kit; Pierce, Rockford, IL).[5]

**Analysis of HTRA1 protein oligomer formation.** HTRA1 trimer formation is mediated by aromatic ring stacking interactions with Y169, F171, and F278.[19] We replaced Y169 and F171 with the nonaromatic residue Glu (Y169E/F171E). We used Y169E/F171E as a negative control and S328A as a positive control for trimer formation.[19] Recombinant HTRA1 protein oligomerization was evaluated by size-exclusion chromatography using a Superdex 200 10/300 GL column (GE Healthcare) on an AKTA FPLC workstation equilibrated with Tris-buffered saline (100 mM Tris-HCl [pH 8.0] and 150 mM NaCl). Before loading, samples were preincubated at 37°C for 30 minutes and injected at 500 μg/mL. The apparent molecular mass of HTRA1 oligomers was calculated based on the calibration curve of the partition coefficient vs log molecular weight. HTRA1 trimers fractionated by size-exclusion chromatography were analyzed by reducing sodium dodecyl sulfate polyacrylamide gel electrophoresis with Coomassie Brilliant Blue staining.

**HTRA1 3D model.** We obtained data for a 3D model of HTRA1 (PDB ID: 3NZI) from the RCSB protein data bank (http://www.rcsb.org/pdb/home/home.do) and created a picture using RasMol software (http://rasmol.org/OpenRasMol.html).[20]

**Statistical analysis.** Statistical analysis was conducted using SPSS version 22 (IBM, Armonk, NY).

## RESULTS

**Frequency of mutations in the *HTRA1* gene in patients with leukoaraiosis.** Among 113 unrelated index patients with severe leukoaraiosis who were younger than 70 years, we found 4 heterozygous missense mutations in the *HTRA1* gene in 6 cases (5.3%); these missense mutations were located in the serine protease domain (figure 1A). Three mutations—p.G283E, p.R302Q, and p.T319I—were novel, and p.P285L was reported as homozygous in one patient with CARASIL and heterozygous in the 65-year-old father of a proband with severe leukoaraiosis.[7] The affected amino acids were either completely or largely conserved among the HTRA1 homologs and orthologs (figure 1B). PolyPhen2 (http://genetics.bwh.harvard.edu/pph/) and sorting intolerant from tolerant (http://sift.jcvi.org/) predicted that the mutations would be damaging; none of these mutations are listed in the Exome Aggregation Consortium (http://exac.broadinstitute.org) (accessed August 21, 2015), the 1000 Genomes project, JSNP (database of gene variations in 934 Japanese subjects),[21] or the 320 in-house Japanese elderly controls.

**Figure 1** Heterozygous *HTRA1* mutations in patients with cerebral small vessel disease

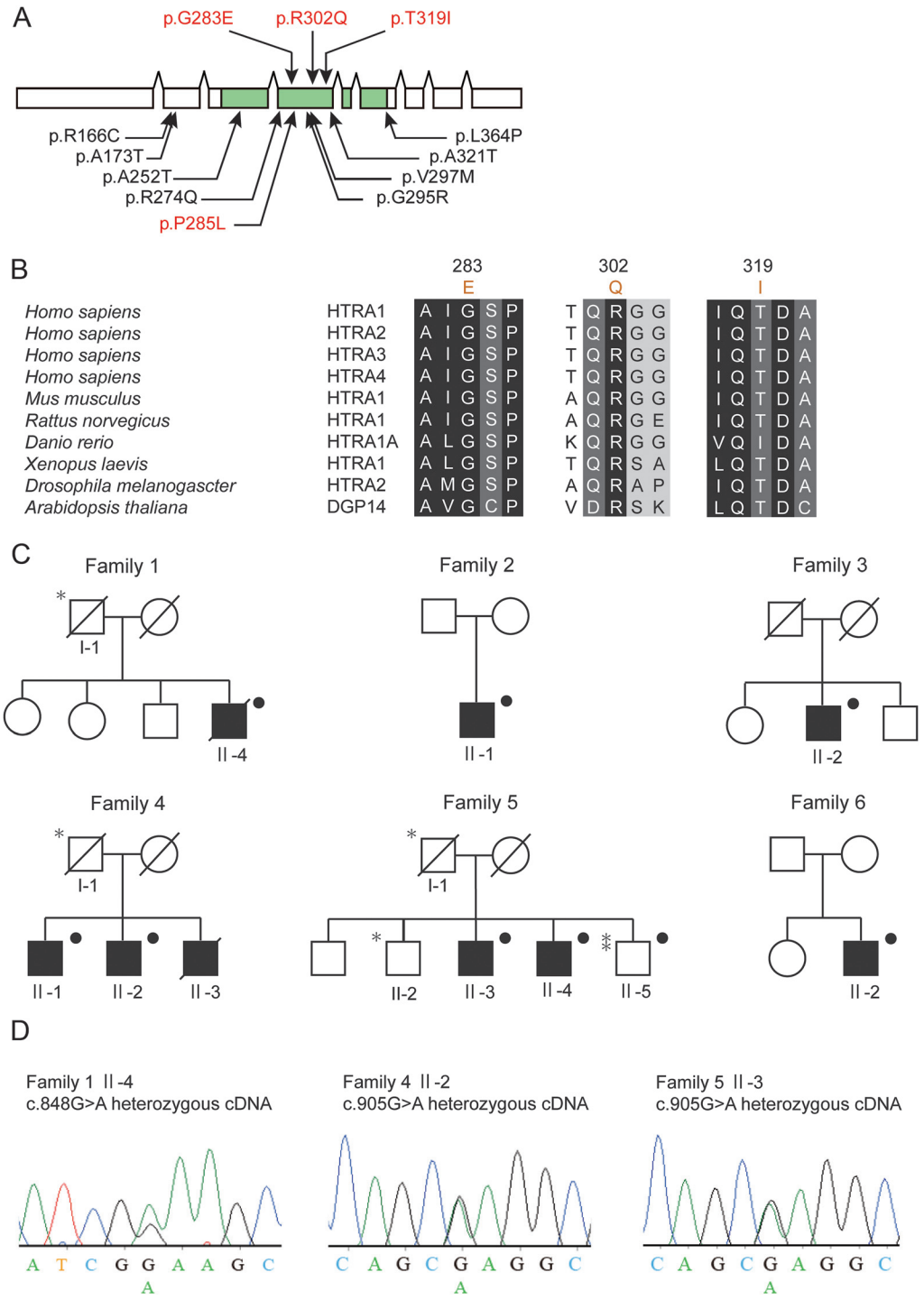


(A) Missense mutations in patients with cerebral autosomal recessive arteriopathy with subcortical infarcts and leukoencephalopathy (CARASIL) or severe leukoaraiosis. The green box shows the protease domain of the *HTRA1* gene. The mutations found in this study are shown in red (p.G283E, p.P285L, p.R302Q, and p.T319I). The mutations shown in black and p.P285L have been associated with CARASIL. (B) Conservation of mutated HTRA1 amino acid residues p.G283E, p.R302Q, and p.T319I. Conserved residues are shaded (black, 100% conserved; dark gray, 80% conserved; gray, 60% conserved). Sequences were obtained from GeneBank (http://www.ncbi.nlm.nih.gov/genbank/). (C) Pedigrees of families with patients with cerebral small vessel disease carrying the heterozygous *HTRA1* mutations. Squares indicate men; circles, women; filled symbols, family members with leukoaraiosis; small filled circles, members undergoing genetic testing. Asterisks represent members with a history of a stroke under 60 years of age; I-1 of family 1, I-1 of family 4, and II-2 of family 5 had cerebral infarction, and I-1 of family 5 had a cerebral hemorrhage. Double asterisks represent the individual with occlusion of the right internal carotid artery who did not have leukoaraiosis or the *HTRA1* mutation. (D) Electropherograms of the sequencing of the HTRA1 complementary DNA derived from the RNA of the lymphocytes from the patients carrying heterozygous *HTRA1* mutations. Both wild-type and mutant alleles are expressed.

Family members in 3 of 6 families had a history of ischemic or hemorrhagic stroke episodes (figure 1C). We obtained DNA from siblings in families 4 and 5. Member II-1 of family 4 and II-4 of family 5 carried heterozygous p.R302Q mutations and had severe leukoaraiosis. To exclude the possibility that transcription from the other allele of the *HTRA1* gene decreases due to mutations in the promoter or introns, we performed sequencing analysis of HTRA1 cDNA obtained from the whole blood samples of member II-4 of family 1, II-2 of family 4, and II-3 of family 5 and confirmed the expression of the other allele of the *HTRA1* gene in these individuals (figure 1D).

**Clinical features of heterozygotes with *HTRA1* missense mutations.** All 8 patients were male and had risk factors for stroke, such as hypertension, a history of heavy alcohol consumption, or a history of smoking (table 1). The mean age at onset was 51.1 years for cognitive impairment and 50.6 years for gait disturbance. Regarding the clinical hallmarks of CARASIL, spondylosis deformans was detected in all cases. Alopecia was detected in 3 patients in the frontal area, as observed in CARASIL (figure 2L), and the mean age at alopecia onset was 26.7 years.

Brain MRI revealed hyperintensities in deep white matter with lacunar infarcts and microbleeds (figure 2, A, B, D–F, and H); white matter lesions in the anterior temporal lobe were milder than those in CARASIL (figure 2, C and G).[22] Brain atrophy presented predominantly in the central region and the frontal lobe. Spinal MRI showed diffuse spondylosis deformans at the cervical spine (figure 2, I and J). Single photon emission CT showed hypoperfusion in the frontal and temporal lobes, thalamus, and brainstem (figure 2K). Histologic findings from autopsied member II-4 of family 1 revealed diffuse and focally intensive myelin pallor in the white matter, but the subcortical U-fibers were spared (figure 2M). The cerebral small arteries showed intimal proliferation, hyaline degeneration of media, and splitting of the internal elastic lamina (figure 2, N–S).

**Protease activity of mutant HTRA1s.** To investigate the functional consequences of *HTRA1* gene mutations, we expressed wild-type HTRA1 tagged with $His_6$ and mutant HTRA1s tagged with $His_6$ and Myc epitopes in FreeStyle 293 cells; we purified HTRA1s from the conditioned media using a Ni column (figure 3A). Protease activity was evaluated using FITC-labeled

**Table 1** Clinical characteristics of the 8 patients with heterozygous *HTRA1* mutations

| | Patients and family | | | | | | | |
|---|---|---|---|---|---|---|---|---|
| Characteristics | II-4, family 1 | II-1, family 2 | II-2, family 3 | II-1, family 4 | II-2, family 4 | II-3, family 5 | II-4, family 5 | II-2, family 6 |
| Stroke history in parent under 60 years of age | Yes | No | No | Yes | Yes | Yes | Yes | Unknown |
| Mutation (amino acid) | p.G283E | p.P285L | p.P285L | p.R302Q | p.R302Q | p.R302Q | p.R302Q | p.T319I |
| Mutation (nucleotide) | c.848G>A | c.854C>T | c.854C>T | c.905G>A | c.905G>A | c.905G>A | c.905G>A | c.956C>T |
| Sex | Male | Male | Male | Male | Male | Male | Male | Male |
| Age at time of study, y | 49 | 51 | 59 | 63 | 57 | 61 | 60 | 57 |
| First stroke episode, age at onset, y | — | 32 | 51 | 63 | — | — | 59 | 53 |
| Cognitive impairment, age at onset, y | 49 | 50 | 53 | 63 | 40 | 44 | 57 | 53 |
| Gait disturbance, age at onset, y | 49 | 32 | 57 | 63 | 40 | 52 | 59 | 53 |
| Alopecia, age at onset, y | — | 20 | — | — | 20 | 40 | — | — |
| Spondylosis deformans | Yes | Yes | Yes | Yes | Yes | Yes | Yes | Yes |
| Pseudobulbar palsy | Yes | No | Yes | No | Yes | No | Yes | Yes |
| Hyperreflexia of limbs | Yes | Yes | Yes | Yes | Yes | Yes | Yes | Yes |
| Babinski reflex | No | Yes | No | Yes | Yes | Yes | Yes | Yes |
| Hypertension | No | Yes | No | Yes | No | No | No | Yes |
| Diabetes mellitus | No | No | No | No | No | No | No | No |
| Dyslipidemia | No | No | No | No | No | No | No | Yes |
| Chronic heart failure | No | No | No | No | No | No | No | No |
| Heavy alcohol consumption | Yes | No | No | No | Yes | Yes | No | No |
| Smoking | Yes | No | Yes | Yes | No | Yes | Yes | No |

**Figure 2** Representative findings of patients carrying the heterozygous *HTRA1* mutations

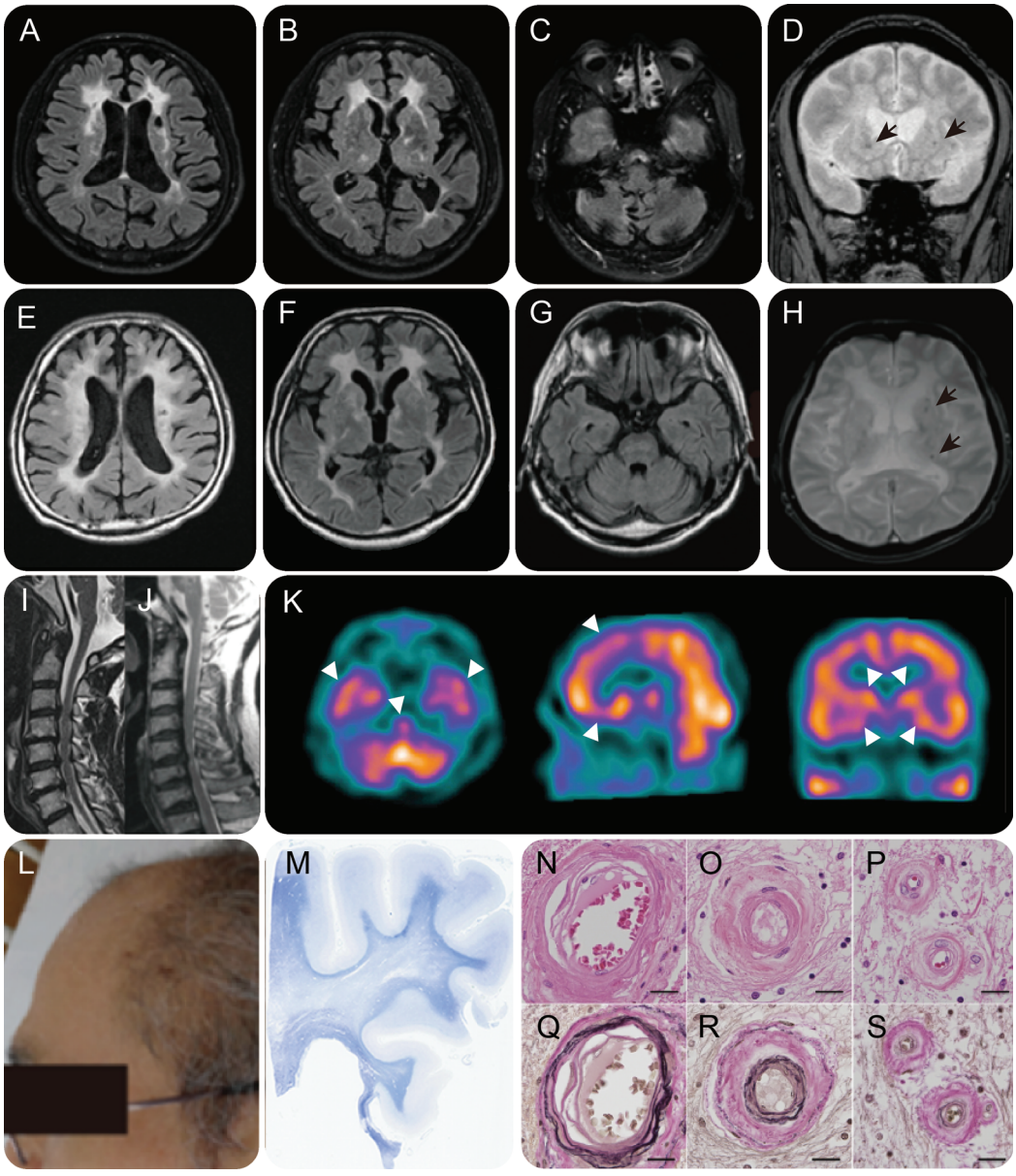


(A–J) MRI of patients carrying the heterozygous *HTRA1* mutations. (A–D, I) Member II-1 of family 2. (E–H, J) Member II-3 of family 5. Fluid-attenuated inversion recovery images of the brain reveal ischemic lesions in the basal ganglia and white matter (A, B, E, F). The anterior temporal lobe was slightly involved (C, G). T2-star gradient echo images reveal microbleeds in the brain parenchyma (D, H, arrows). T2-weighted cervical MRI reveal spondylotic changes from C4 to C7 (I, J). (K) Hypoperfusion in the frontal lobe, temporal lobe, thalamus, and pons on 99mTc ethyl cysteinate dimer single photon emission CT images (regional cerebral blood flow [CBF] relative to cerebellar CBF using 3DSRT[30]; pons: 0.34, rectal gyrus: 0.54, orbital gyrus: 0.71, superior frontal gyrus: 0.91, inferior temporal gyrus: 0.78, parahippocampal gyrus: 0.86, thalamus: 0.92) (arrowheads; II-3 in family 5). (L) Diffuse hair loss of the head was observed in member II-3 of family 5 at 61 years of age. (M) Coronal section of the frontal lobe stained with Luxol fast blue from member II-4 of family 1. Note the pale staining in the deep white matter, indicating myelin loss. (N, Q, O, R) Cerebral small arteries show marked intimal thickening, narrowing of the lumen, hyalinosis, and splitting of the internal elastic membrane. (N–P) Arteries in the white matter stained with hematoxylin & eosin. (Q–S) Arteries in the white matter stained with elastica van Gieson stain; (N–S) scale bar, 20 μm.

casein as the substrate.[5] We used S328A HTRA1, an introduced mutation at the active site, as a negative control.[18] As we have shown previously, the protease activities in A252T and V297M HTRA1s, observed in CARASIL, were lower than that of wild-type HTRA1 but higher than that of S328A HTRA1 (figure 3B).[5] The protease activity of R274Q HTRA1, also observed in CARASIL,[11] was markedly decreased and comparable to that of S328A HTRA1 (figure 3B). G283E, P285L, R302Q, and T319I HTRA1s, the mutant HTRA1s observed in the manifesting heterozygotes, had markedly decreased protease activities, comparable to that of S328A HTRA1 (figure 3B).

**Figure 3** Functional consequences of mutant HTRA1s found in heterozygotes

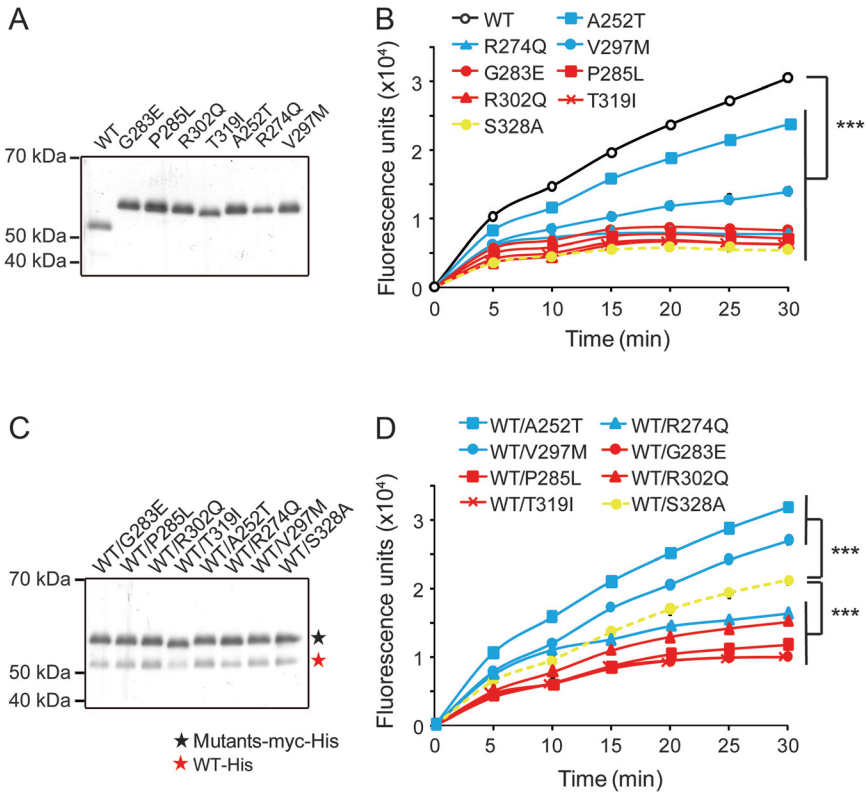


(A, B) Protease activity of the HTRA1s. (A) The HTRA1 proteins used in the protease assay. Human HTRA1 proteins purified from the conditioned medium of FreeStyle 293 cells transfected with $His_6$-tagged full-length wild-type HTRA1 or each myc-$His_6$-tagged mutant HTRA1 expression plasmid. Equal amounts of HTRA1 proteins were loaded onto sodium dodecyl sulfate polyacrylamide gel electrophoresis (SDS-PAGE) gels and visualized by Coomassie Brilliant Blue staining. T319I HTRA1 is smaller than the others probably due to nonglycosylation at T319. The wild-type HTRA1 band decreased more than the mutant HTRA1 bands due to the autodegradation capacity of wild-type HTRA1. The protease capacity remained in these autodegraded products.[24–26] (B) Protease assay for HTRA1 proteins. Fluorescein isothiocyanate (FITC)–labeled casein was incubated with human HTRA1 proteins. The black line indicates wild-type HTRA1; dashed yellow line: S328A, which abolished the protease activity; blue lines: HTRA1 mutants associated with CARASIL; red lines: HTRA1 mutants found in patients with cerebral small vessel disease (CSVD) in the heterozygote state. The mean values from 5 independent experiments are shown. I-bars indicate the SEM. Group comparisons were performed with one-way analysis of variance, followed by the Bonferroni post hoc test using fluorescence values after 30 minutes. ***$p < 0.001$. The protease activities of each HTRA1 mutant, relative to wild-type HTRA1, are as follows: A252T, 0.78; R274Q, 0.26; V297M, 0.46; G283E, 0.27; P285L, 0.23; R302Q, 0.21; T319I, 0.21; S328A, 0.18. (C, D) Protease activity of the HTRA1 complexes. (C) The HTRA1 protein complexes used in the protease assay. Human HTRA1 protein complexes purified from the conditioned media of FreeStyle 293 cells cotransfected with $His_6$-tagged wild-type HTRA1 and each myc-$His_6$-tagged mutant HTRA1 expression plasmid at equal molar amounts. Equal amounts of HTRA1 proteins were loaded onto SDS-PAGE gels and visualized by Coomassie Brilliant Blue staining. The band from wild-type HTRA1 decreased more than those of the mutants due to wild-type HTRA1's autodegradation capacity. (D) Protease assay for HTRA1 protein complexes. FITC-labeled casein was incubated with human HTRA1 protein complexes. The dashed yellow line indicates the complex consisting of wild-type and S328A HTRA1; blue lines: the complex consisting of wild-type and each mutant HTRA1 associated with cerebral autosomal recessive arteriopathy with subcortical infarcts and leukoencephalopathy; red lines: the complex consisting of wild-type and each mutant HTRA1 found in patients with CSVD in the heterozygous state. The mean values from 5 independent experiments are shown. I-bars indicate the SEM. Group comparisons were performed with one-way analysis of variance, followed by the Bonferroni post hoc test using fluorescence values after 30 minutes. ***$p < 0.001$. The protease activities of the complexes consisting of wild-type HTRA1 and each HTRA1 mutant relative to that of wild-type HTRA1 and S328A are as follows: A252T, 1.50; R274Q, 0.77; V297M, 1.27; G283E, 0.47; P285L, 0.56; R302Q, 0.71; T319I, 0.48.

**Inhibition of wild-type HTRA1 activity by mutant HTRA1s.** HTRA1 exists as a trimer and is activated by substrate-induced cascade transmission to an adjacent HTRA1 subunit.[19,23] Therefore, we hypothesized that the mutant HTRA1s observed in manifesting heterozygotes inhibit wild-type HTRA1 protease activity as a dominant-negative effect. To investigate this possibility, we coexpressed wild-type and each mutant HTRA1 in FreeStyle 293 cells and purified these HTRA1s as a mixture. The amount of wild-type HTRA1 was less than that of the mutant HTRA1s due to autolysis of wild-type HTRA1 (figure 3C).[24–26] To investigate the effect of the mutant HTRA1s on wild-type HTRA1, we selected

a mixture of wild-type and S328A HTRA1s as a control; S328A HTRA1 is catalytically inactive but forms the proper trimer.[18,19] Under identical substrate and protease concentrations, the protease activity of the HTRA1 mixture of wild-type and A252T or V297M HTRA1s, 2 mutations observed in CARASIL, was higher than that of the control mixture; in contrast, the protease activities of all the other HTRA1 mixtures (figure 3D) were lower than that of the control mixture, indicating that these HTRA1 mutants inhibit the protease activity of wild-type HTRA1.

**The oligomeric property for mutant HTRA1s.** Therefore, we hypothesized that the HTRA1 mutants observed in manifesting heterozygotes decrease wild-type HTRA1 protease activity through an impairment of the trimer-associated activation cascade. We investigated the oligomeric properties of each HTRA1 by size-exclusion chromatography. As a control for monomers, we introduced mutations into 2 of the 3 amino acids that are essential for stable trimer formation: Y169E/F171E HTRA1.[19] Because wild-type HTRA1 is autolyzed,[24–26] we used S328A HTRA1 as a control for trimers, as previously reported.[19] Size-exclusion chromatography revealed that S328A HTRA1 eluted at approximately 295 kDa, whereas Y169E/F171E mainly eluted as a ~97 kDa monomer (figure 4A).

Next, we investigated the oligomeric properties of mutant HTRA1s. Among the mutations observed in CARASIL, A252T and V297M eluted as ~295 kDa trimers (figure 4B). R274Q HTRA1, which inhibited wild-type HTRA1 activity, eluted as a ~97 kDa monomer (figure 4B). Among the mutations observed in manifesting heterozygotes, P285L and R302Q HTRA1s eluted as trimers (figure 4C), whereas T319I and G283E HTRA1s broadly eluted from 75 to 440 kDa, suggesting that these HTRA1 mutants fail to form trimers due to improper folding (figure 4C). To investigate whether the monomeric HTRA1s inhibit wild-type HTRA1 activity, we investigated the protease activity of Y169E/F171E HTRA1. Y169E/F171E HTRA1 showed markedly decreased protease activity, comparable to that of S328A HTRA1 (figure 4D); the mixture of wild-type and Y169E/F171E HTRA1s showed lower protease activity than that of the wild-type and S328A HTRA1s mixture, suggesting that HTRA1s that cannot form trimers inhibit wild-type HTRA1 protease activity (figure 4E).

**DISCUSSION** We show the heterozygous missense mutations p.G283E, p.P285L, p.R302Q, and p.T319I in the *HTRA1* gene in 8 patients with symptomatic CSVD. We conclude that these mutations contribute to CSVD pathogenesis because these mutations were not found in controls; cosegregation between leukoaraiosis and the p.R302Q mutation was demonstrated in 2 separate families; and these mutant HTRA1s showed markedly decreased protease activities. Our observations support the finding that the heterozygous mutations in *HTRA1* are associated with CSVD. Moreover, we demonstrated that the pathologic findings of the patients with the heterozygous p.G283E mutation resemble CARASIL.[5,10,27,28] The strength of our study is that we have demonstrated that the mutant HTRA1s associated with manifesting heterozygotes have dominant-negative effects on wild-type HTRA1 protease activity, indicating that the HTRA1 protease activities of manifesting heterozygotes might be less than those of heterozygotes carrying the p.R302ter or p.R370ter mutations that do not develop symptomatic CSVD.[5,15] In contrast, A252T or V297M HTRA1s, observed in CARASIL,[5] did not inhibit wild-type HTRA1 activity; this difference might explain why some mutations in *HTRA1* are associated with symptomatic CSVD in heterozygotes.

We further investigated the mechanism of the dominant-negative effect from the analysis of oligomeric states. These mutants have 3 distinct oligomeric states: trimer formation (p.P285L and p.R302Q), impaired trimer formation by improper folding (p.T319I and p.G283E), and monomer (p.R274Q). The wild-type HTRA1 monomers form a trimer; it has been speculated that each HTRA1 is activated by substrate-induced cascade transmission to an adjacent HTRA1 subunit.[19,23] Substrate binding to the sensor loop L3 domain stimulates loop LD of the neighboring HTRA1, inducing the active conformation. Each activated HTRA1 subunit then digests substrate independently. The sensor loop L3 consists of amino acids 301 to 314 and the activation loop LD consists of amino acids 283 to 291 (figure 4F)[19]; the P285L and R302Q HTRA1s have mutations within the LD and L3 domains, respectively. Thus these mutant HTRA1s might interfere with the trimer-associated activation cascade, resulting in a failure of activation of the wild-type HTRA1 involved in the trimer. In contrast, the A252T and V297M HTRA1s, which are observed in CARASIL and form trimers, have mutations outside the LD and L3 domains. Therefore, although these mutants are catalytically inactive, they may not inhibit the activity of wild-type HTRA1 involved in a trimer. Interestingly, p.S284R, p.S284G, p.P285Q, and p.F286V, identified by Verdura et al.[9] in heterozygous patients with CSVD, are also located within the LD domain, further supporting our hypothesis.

The other mutants failed to form trimers. The G283E and T319I HTRA1s failed to achieve proper folding and, consequently, failed to form trimers. The

**Figure 4** Oligomeric states of mutant HTRA1 proteins

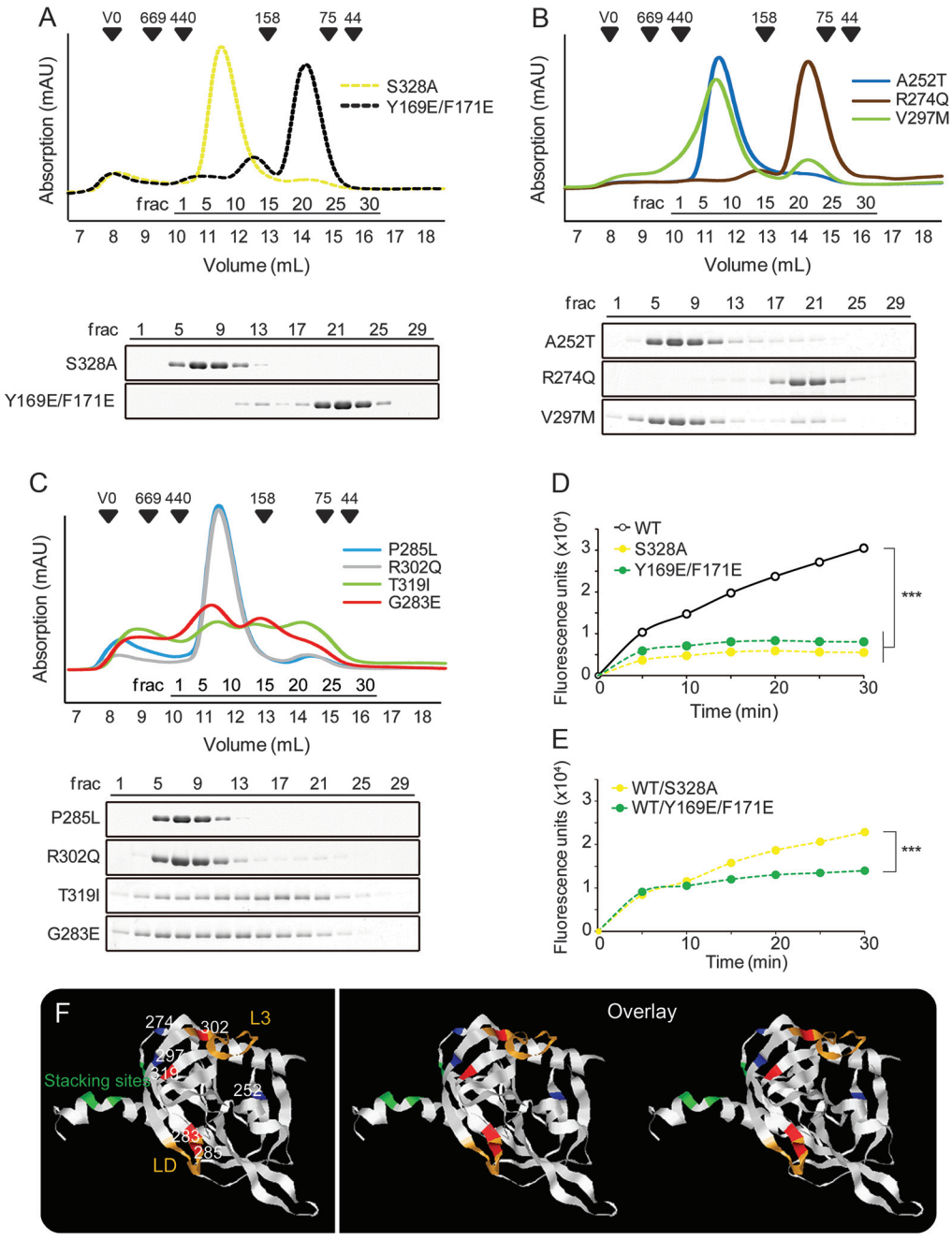


(A) Oligomeric state analysis of the HTRA1 trimer and monomer by size-exclusion chromatography. Upper panel: Elution profile of S328A or Y169E/F171E HTRA1 from the Superdex 200 10/300 GL column. The column was calibrated with standard proteins (thyroglobulin 669 kDa, ferritin 440 kDa, aldolase 158 kDa, conalbumin 75 kDa, and ovalbumin 44 kDa). The void volume (Vo) was determined with dextran 2000. The Vo of the column and the elution volumes of standard marker proteins are indicated by black arrowheads. Lower panel: aliquots of the size-exclusion chromatography fractions separated by sodium dodecyl sulfate polyacrylamide gel electrophoresis (SDS-PAGE) and visualized by Coomassie Brilliant Blue staining. (B, C) Oligomeric state analysis of each mutant HTRA1 protein by size-exclusion chromatography. (B) HTRA1 mutants associated with cerebral autosomal recessive arteriopathy with subcortical infarcts and leukoencephalopathy. (C) HTRA1 mutants found in patients with CSVD in heterozygotes. Upper panel: elution profiles of the HTRA1 mutants. Lower panel: aliquots of the size-exclusion chromatography fractions separated by SDS-PAGE and visualized by Coomassie Brilliant Blue staining. (D) Protease assay for Y169E/F171E HTRA1. Fluorescein isothiocyanate (FITC)–labeled casein was incubated with HTRA1 proteins. Black line indicates wild-type (wild-type) HTRA1; yellow dashed line: S328A, which abolished the protease activity; green dashed line: Y169E/F171E. (E) Protease assay for wild-type and Y169E/F171E HTRA1 complexes. FITC-labeled casein was incubated with human HTRA1 protein complexes. The dashed yellow line indicates the complex consisting of wild-type and S328A HTRA1s; green dashed line: the complex consisting of wild-type and Y169E/F171E HTRA1s. The mean values from 5 independent experiments are shown. I-bars indicate the SEM. Group comparisons were performed with one-way analysis of variance, followed by the Bonferroni post hoc test using fluorescence values after 30 minutes. ***$p < 0.001$. (F) The HTRA1 monomer is displayed as a ribbon diagram with RasMol.[20] The structure reference dataset of HTRA1 from the RCSB Protein Data Bank (PDB ID: 3NZI) was introduced. The sensor loop L3 (amino acids 301 to 314) and the activation loop LD (amino acids 283 to 291) are highlighted in orange. The amino acids that mediate HTRA1 trimer formation (Y169, F171, and F278) are highlighted in green. The positions of the amino acids that were substituted in the mutations found in homozygous patients are highlighted in blue, and those found in heterozygous patients are highlighted in red.

R274Q HTRA1, observed in CARASIL,[11] was observed as a monomer; R274Q is located near F278, which is a core residue for trimer formation.[19] We demonstrated that the artificial HTRA1mutant Y169E/F171E, which was observed as a monomer, also inhibited wild-type HTRA1 activity. A similar mechanism was shown in the dominant-negative effect exerted by the p.G278R receptor activator of nuclear factor kappa-B ligand (RANKL) variant.[29] The G278R RANKL monomers failed to assemble into homotrimers and interact with wild-type RANKL, resulting in a dominant-negative effect on trimerization[29]; we speculate that these HTRA1 mutants might interfere with the trimerization of wild-type HTRA1 in a similar manner, and this possibility should be evaluated in future studies. Although the clinical spectrum has not been assessed in p.R274Q heterozygotes,[11] it would be important to assess whether these individuals develop symptomatic CSVD. Interestingly, p.R166L and p.A173P, reported by Verdura et al.[9] in heterozygous patients with CSVD, are also located near Y169 or F171, which are essential for trimer stabilization.[19]

The clinical features of manifesting heterozygotes with *HTRA1* mutations are a weak phenocopy of CARASIL; the age at neurologic deficit onset was older and the hyperintensities on MRI of white matter were less severe than in CARASIL.[4,22] The frequency of alopecia was 37.5%, compared to 69.2% in CARASIL[4]; however, spondylosis deformans was observed in all individuals, suggesting that HTRA1 activity fundamentally contributes to the pathogenesis of spondylosis. For sex and environmental factors, all of our patients were male and had risk factors for stroke. The frequency of heterozygous mutation in the *HTRA1* gene is 10.0% for males with leukoaraiosis. Although male predominance has not been identified in genetically diagnosed CARASIL,[4] this sex disparity has been proposed in clinically diagnosed CARASIL.[2] Recently, Verdura et al.[9] reported 11 heterozygous *HTRA1* mutations in patients with CSVD; none of these patients had early-onset alopecia or spondylosis, there was no sexual predominance, and 5 patients did not show hypertension. To reveal the clinical feature for heterozygotes with *HTRA1* mutations, we have to accumulate more clinical information from the relatives of patients with CARASIL.

Because of the autolytic property of wild-type HTRA1,[24–26] the amount of wild-type HTRA1 is lower than that of the mutant HTRA1s in coexpression experiments. Therefore, we must consider the possibility that the excess amount of mutant HTRA1s exhibited a dominant-negative effect in this study; however, we consider the experiment in this report appropriate to evaluate the effects of mutant HTRA1s on wild-type HTRA1 activity. We compared the activities of mutant HTRA1s to that of the catalytically inactive S328A HTRA1, and the amounts of wild-type HTRA1 in each mixture consisting of wild-type and mutant HTRA1s appeared to be identical. Moreover, we carefully adjusted the amounts of plasmids, HTRA1 mixtures, and substrates in this study.

The limitation of our study is that we were not able to investigate all of the asymptomatic siblings in the investigated families; larger studies for siblings and families are required to extend our findings. In addition, several *HTRA1* mutations observed in heterozygotes with symptomatic CSVD are not consistent with our hypothesis; however, the protease activity did not decrease or was not evaluated in these mutants (p.S121R, p.A123S, p.R133G, p.D450H, and c.973-1G>A).[9] Therefore, the molecular mechanism for these mutations should be evaluated.

We found that HTRA1 mutants associated with manifesting heterozygotes exerted a dominant-negative

## Comment: Autosomal dominant small vessel disease due to heterozygous *HTRA1* mutations

Cerebral autosomal recessive arteriopathy with subcortical infarcts and leukoencephalopathy (CARASIL), a recessive form of small vessel disease (SVD) caused by mutations in the serine protease gene *HTRA1*, was previously considered a rare, early-onset form of SVD, in which biallelic mutations result in a loss of HTRA1 activity.

However, this study reports 4 heterozygous *HTRA1* mutations—G283E, R302Q, T319I, and P285L—as causes of SVD with a dominant inheritance pattern.[1] The results are in accordance with an earlier study that reported 11 other heterozygous *HTRA1* mutations.[2] In addition, this study indicates deficient protease activity caused by dominant negative mutations or inhibition of HTRA1 trimer stabilization as plausible mechanisms. Despite the remaining possibility of folding defects in individual HTRA1 monomers, this study uncovers a novel mechanism of SVD. The frequency of dominant mutations is predicted to be much higher than recessive inheritance. To date, we may have overlooked heterozygous carriers due to their weaker phenotype of CARASIL symptoms. These include older onset of stroke and dementia,[1,2] lower frequency of extraneurologic symptoms such as alopecia[1,2] and spondylosis,[2] and less severe white matter hyperintensities on MRI.[1]

Surprisingly, most factors involved in SVD have remained elusive.[3] Even vascular risk factors such as hypertension explain only minor proportions (~2%) of the variance in white matter hyperintensities. The current study has therefore advanced our knowledge by identifying an important contributor to SVD with white matter hyperintensities. However, questions remain to be resolved, including whether and how heterozygous *HTRA1* mutations interact with environmental factors, which downstream signaling pathways are affected, and which cell types (e.g., pericytes or oligodendrocytes) are subsequently damaged. The findings provided in this study will aid the early diagnosis of SVD and, along with further research, will help untangle the multiple but interrelated pathways of SVD.


1. Nozaki H, Kato T, Nihonmatsu M, et al. Distinct molecular mechanisms of *HTRA1* mutants in manifesting heterozygotes with CARASIL. Neurology 2016;86:1964–1974.
2. Verdura E, Hervé D, Scharrer E, et al. Heterozygous HTRA1 mutations are associated with autosomal dominant cerebral small vessel disease. Brain 2015;138:2347–2358.
3. Ihara M, Yamamoto Y. Emerging evidence for pathogenesis of sporadic cerebral small vessel disease. Stroke 2016;47:554–560.



*Masafumi Ihara, MD, PhD, FACP*

From the Division of Neurology, Department of Stroke and Cerebrovascular Diseases, National Cerebral and Cardiovascular Center, Osaka, Japan.


Study funding: No targeted funding reported.
Disclosure: The author reports no disclosures relevant to the manuscript. Go to Neurology.org for full disclosures.

effect. These mutant HTRA1s were classified into 2 types: mutations resulting in an impairment of HTRA1's activation cascade or stable trimer formation. These biochemical features, which are distinct from the mutant HTRA1s observed in CARASIL, will provide useful information to estimate the risk for development of symptomatic CSVD for each *HTRA1* mutation and allow better approaches for individuals and families with *HTRA1* mutations.

## AUTHOR CONTRIBUTIONS

Hiroaki Nozaki: drafted/revised the manuscript for content, study concept, design, acquired, analyzed, and interpreted data, and obtained funding. Taisuke Kato: drafted/revised the manuscript for content, study concept, design, and acquired, analyzed, and interpreted data. Megumi Nihonmatsu: acquired data. Yohei Saito: acquired data. Ikuko Mizuta: acquired, analyzed, and interpreted data. Tomoko Noda: acquired data. Ryoko Koike: acquired data. Kazuhide Miyazaki: acquired data. Muichi Kaito: acquired data. Shoici Ito: acquired data. Masahiro Makino: acquired data. Akihide Koyama: acquired, analyzed and interpreted data. Atsushi Shiga: acquired, analyzed and interpreted data. Masahiro Uemura: acquired data. Yumi Sekine: acquired data. Ayuka Murakami: acquired data. Suzuko Moritani: acquired, analyzed and interpreted data. Kenju Hara: drafted/revised the manuscript for content, and acquired, analyzed, and interpreted data. Akio Yokoseki: acquired data and obtained funding. Ryoso Kuwano: acquired data. Naoto Endo: acquired data and obtained funding. Takeshi Momotsu: acquired data. Mari Yoshida: drafted the manuscript for content and obtained, analyzed and interpreted data. Masatoyo Nishizawa: drafted/revised the manuscript for content, study concept, design, and analyzed and interpreted data. Toshiki Mizuno: drafted/revised the manuscript for content, study concept, design, and acquired, analyzed, and interpreted data. Osamu Onodera: drafted/revised the manuscript for content, study concept, design, acquired, analyzed, and interpreted data, and obtained funding.


## ACKNOWLEDGMENT

The authors thank the patients and families who provided the data for this investigation. They also thank Haruka Ishidaira, Eri Furukawa, Miyuki Tsuchiya, and Sachiko Hirokawa for technical assistance.

## STUDY FUNDING

This research was supported by: a grant-in-aid for Scientific Research on Innovative Areas (Brain Protein Aging and Dementia Control) (26117006) from MEXT; a grant-in-aid for Medical Research from the Takeda Science Foundation; a grant-in-aid for Scientific Research (B) (25293200) from the Japan Society for the Promotion of Science; a grant-in-aid for Young Scientist (B) (23790983); a grant-in-aid for the Research Committee for Hereditary Cerebral Small Vessel Disease; a grant-in-aid for Comprehensive Research on Disability from Health and Welfare from the Ministry of Health, Labor, and Welfare, Japan; a grant-in-aid for Project in Sado for Total Health from the Ministry of Education, Culture, Sports, Science, and Technology of Japan; a Yujin Memorial Grant from Yujin Society; and a grant-in-aid from the Cardiovascular Research Fund, Tokyo, Japan.


## DISCLOSURE

H. Nozaki, T. Kato, M. Nihonmatsu, Y. Saito, I. Mizuta, T. Noda, R. Koike, K. Miyazaki, M. Kaito, S. Ito, M. Makino, A. Koyama, A. Shiga, M. Uemura, Y. Sekine, A. Murakami, S. Moritani, K. Hara, A. Yokoseki, R. Kuwano, N. Endo, T. Momotsu, M. Yoshida, M. Nishizawa, and T. Mizuno report no disclosures relevant to the manuscript. O. Onodera received research support from the Takeda Science Foundation. Go to Neurology.org for full disclosures.


*Received September 8, 2015. Accepted in final form February 4, 2016.*


## REFERENCES


1. Fukutake T, Hirayama K. Familial young-adult-onset arteriosclerotic leukoencephalopathy with alopecia and lumbago without arterial hypertension. Eur Neurol 1995;35:69–79.
2. Fukutake T. Cerebral autosomal recessive arteriopathy with subcortical infarcts and leukoencephalopathy (CARASIL): from discovery to gene identification. J Stroke Cerebrovasc Dis 2011;20:85–93.
3. Onodera O, Nozaki H, Fukutake T. In: Pagon RA, Adam MP, Ardinger HH, et al, editors. GeneReviews®. Seattle: University of Washington; 1993–2014.
4. Nozaki H, Nishizawa M, Onodera O. Features of cerebral autosomal recessive arteriopathy with subcortical infarcts and leukoencephalopathy. Stroke 2014;45:3447–3453.
5. Hara K, Shiga A, Fukutake T, et al. Association of HTRA1 mutations and familial ischemic cerebral small-vessel disease. N Engl J Med 2009;360:1729–1739.
6. Mendioroz M, Fernandez-Cadenas I, Del Rio-Espinola A, et al. A missense *HTRA1* mutation expands CARASIL syndrome to the Caucasian population. Neurology 2010;75:2033–2035.
7. Chen Y, He Z, Meng S, Li L, Yang H, Zhang X. A novel mutation of the high-temperature requirement A serine peptidase 1 (*HTRA1*) gene in a Chinese family with cerebral autosomal recessive arteriopathy with subcortical infarcts and leukoencephalopathy (CARASIL). J Int Med Res 2013;41:1445–1455.
8. Bianchi S, Di Palma C, Gallus GN, et al. Two novel *HTRA1* mutations in a European CARASIL patient. Neurology 2014;82:898–900.
9. Verdura E, Herve D, Scharrer E, et al. Heterozygous *HTRA1* mutations are associated with autosomal dominant cerebral small vessel disease. Brain 2015;138:2347–2358.
10. Yanagawa S, Ito N, Arima K, Ikeda S. Cerebral autosomal recessive arteriopathy with subcortical infarcts and leukoencephalopathy. Neurology 2002;58:817–820.
11. Nishimoto Y, Shibata M, Nihonmatsu M, et al. A novel mutation in the *HTRA1* gene causes CARASIL without alopecia. Neurology 2011;76:1353–1355.
12. Wang XL, Li CF, Guo HW, Cao BZ. A novel mutation in the *HTRA1* gene identified in Chinese CARASIL pedigree. CNS Neurosci Ther 2012;18:867–869.
13. Menezes Cordeiro I, Nzwalo H, Sa F, et al. Shifting the CARASIL paradigm: report of a non-Asian family and literature review. Stroke 2015;46:1110–1112.
14. Khaleeli Z, Jaunmuktane Z, Beaufort N, et al. A novel *HTRA1* exon 2 mutation causes loss of protease activity in a Pakistani CARASIL patient. J Neurol 2015;262:1369–1372.
15. Bayrakli F, Balaban H, Gurelik M, Hizmetli S, Topaktas S. Mutation in the HTRA1 gene in a patient with degenerated spine as a component of CARASIL syndrome. Turk Neurosurg 2014;24:67–69.
16. Vernooij MW, Ikram MA, Tanghe HL, et al. Incidental findings on brain MRI in the general population. N Engl J Med 2007;357:1821–1828.
17. Fazekas F, Kleinert R, Offenbacher H, et al. The morphologic correlate of incidental punctate white matter hyperintensities on MR images. AJNR Am J Neuroradiol 1991;12:915–921.
18. Hu SI, Carozza M, Klein M, Nantermet P, Luk D, Crowl RM. Human HtrA, an evolutionarily conserved

serine protease identified as a differentially expressed gene product in osteoarthritic cartilage. J Biol Chem 1998;273:34406–34412.
19. Truebestein L, Tennstaedt A, Monig T, et al. Substrate-induced remodeling of the active site regulates human HTRA1 activity. Nat Struct Mol Biol 2011;18:386–388.
20. Sayle RA, Milner-White EJ. RASMOL: biomolecular graphics for all. Trends Biochem Sci 1995;20:374.
21. Hirakawa M, Tanaka T, Hashimoto Y, Kuroda M, Takagi T, Nakamura Y. JSNP: a database of common gene variations in the Japanese population. Nucleic Acids Res 2002;30:158–162.
22. Nozaki H, Sekine Y, Fukutake T, et al. Characteristic features and progression of abnormalities on MRI for CARASIL. Neurology 2015;85:459–463.
23. Clausen T, Kaiser M, Huber R, Ehrmann M. HTRA proteases: regulated proteolysis in protein quality control. Nat Rev Mol Cell Biol 2011;12:152–162.
24. Lorenzi T, Marzioni D, Giannubilo S, et al. Expression patterns of two serine protease HtrA1 forms in human placentas complicated by preeclampsia with and without intrauterine growth restriction. Placenta 2009;30:35–40.
25. Lorenzi T, Lorenzi M, Altobelli E, et al. HtrA1 in human urothelial bladder cancer: a secreted protein and a potential novel biomarker. Int J Cancer 2013;133:2650–2661.
26. Risor MW, Poulsen ET, Thomsen LR, et al. The autolysis of human HtrA1 is governed by the redox state of its N-terminal domain. Biochemistry 2014;53:3851–3857.
27. Arima K, Yanagawa S, Ito N, Ikeda S. Cerebral arterial pathology of CADASIL and CARASIL (Maeda syndrome). Neuropathology 2003;23:327–334.
28. Oide T, Nakayama H, Yanagawa S, Ito N, Ikeda S, Arima K. Extensive loss of arterial medial smooth muscle cells and mural extracellular matrix in cerebral autosomal recessive arteriopathy with subcortical infarcts and leukoencephalopathy (CARASIL). Neuropathology 2008;28:132–142.
29. Douni E, Rinotas V, Makrinou E, et al. A RANKL G278R mutation causing osteopetrosis identifies a functional amino acid essential for trimer assembly in RANKL and TNF. Hum Mol Genet 2012;21:784–798.
30. Takeuchi R, Yonekura Y, Matsuda H, Konishi J. Usefulness of a three-dimensional stereotaxic ROI template on anatomically standardised 99mTc-ECD SPET. Eur J Nucl Med Mol Imaging 2002;29:331–341.